

Dinuclear Oxidative Addition of N–H and S–H Bonds at Chromium. Reaction of $\cdot\text{Cr}(\text{CO})_3(\text{C}_5\text{Me}_5)$ with $\{\text{o}-(\text{HA})\text{C}_6\text{H}_4\text{S}-\text{Cr}(\text{CO})_3(\text{C}_5\text{Me}_5)\}$ (A = S, NH) Yielding $[\eta^2-\text{o}-(\mu\text{-A})\text{C}_6\text{H}_4\text{S}-\text{Cr}(\text{C}_5\text{Me}_5)]_2$ and $\text{H}-\text{Cr}(\text{CO})_3(\text{C}_5\text{Me}_5)$

Kengkaj Sukcharoenphon,[†] Telvin D. Ju,[†] Khalil A. Abboud,[‡] and Carl D. Hoff*[†]

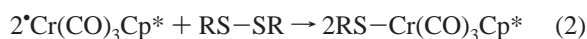
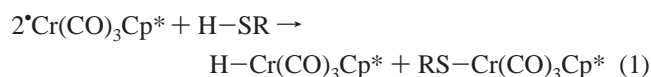
Department of Chemistry, University of Miami, Coral Gables, Florida 33124, and
Department of Chemistry, University of Florida, Gainesville, Florida 32611

Received August 5, 2002

Reaction of the 17-electron radical $\cdot\text{Cr}(\text{CO})_3\text{Cp}^*$ ($\text{Cp}^* = \text{C}_5\text{Me}_5$) with 0.5 equiv of 2-aminophenyl disulfide [$(\text{o}-\text{H}_2\text{N}-\text{NC}_6\text{H}_4)_2\text{S}_2$] results in rapid oxidative addition to form the initial product $(\text{o}-\text{H}_2\text{N})\text{C}_6\text{H}_4\text{S}-\text{Cr}(\text{CO})_3\text{Cp}^*$. Addition of a second equivalent of $\cdot\text{Cr}(\text{CO})_3\text{Cp}^*$ to this solution results in the formation of $\text{H}-\text{Cr}(\text{CO})_3\text{Cp}^*$ as well as $1/2[\eta^2-\text{o}-(\mu\text{-NH})\text{C}_6\text{H}_4\text{S}\}\text{CrCp}^*]_2$. Spectroscopic data show that $(\text{o}-\text{H}_2\text{N})\text{C}_6\text{H}_4\text{S}-\text{Cr}(\text{CO})_3\text{Cp}^*$ loses CO to form $\{\eta^2-(\text{o}-\text{H}_2\text{N})-\text{C}_6\text{H}_4\text{S}\}\text{Cr}(\text{CO})_2\text{Cp}^*$. Attack on the N–H bond of the coordinated amine by $\cdot\text{Cr}(\text{CO})_3\text{Cp}^*$ provides a reasonable mechanism consistent with the observation that both chelate formation and oxidative addition of the N–H bond are faster under argon than under CO atmosphere. The N–H bonds of uncoordinated aniline do not react with $\cdot\text{Cr}(\text{CO})_3\text{Cp}^*$. Reaction of the 2 mol of $\cdot\text{Cr}(\text{CO})_3\text{Cp}^*$ with 1,2-benzene dithiol [$1,2-\text{C}_6\text{H}_4(\text{SH})_2$] yields the initial product $(\text{o}-\text{HS})\text{C}_6\text{H}_4\text{S}-\text{Cr}(\text{CO})_3\text{Cp}^*$ and 1 mol of $\text{H}-\text{Cr}(\text{CO})_3\text{Cp}^*$. Addition of 1 equiv more of $\cdot\text{Cr}(\text{CO})_3\text{Cp}^*$ to this solution also results in the formation of 1 equiv of $\text{H}-\text{Cr}(\text{CO})_3\text{Cp}^*$, as well as the dimeric product $1/2[\eta^2-\text{o}-(\mu\text{-S})\text{C}_6\text{H}_4\text{S}\}\text{CrCp}^*]_2$. This reaction also occurs more rapidly under Ar than under CO, consistent with intramolecular coordination of the second thiol group prior to oxidative addition. The crystal structures of $[\eta^2-\text{o}-(\mu\text{-NH})\text{C}_6\text{H}_4\text{S}\}\text{CrCp}^*]_2$ and $[\eta^2-\text{o}-(\mu\text{-S})\text{C}_6\text{H}_4\text{S}\}\text{CrCp}^*]_2$ are reported.

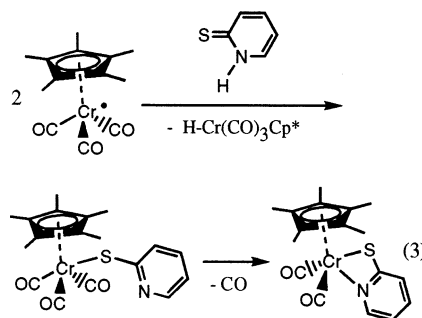
Introduction

Recent work in our laboratory has investigated the mechanism of reaction of the 17-electron organometallic radical $\cdot\text{Cr}(\text{CO})_3\text{Cp}^*$ ($\text{Cp}^* = \text{C}_5\text{Me}_5$) with the thiols¹ and disulfides² as shown in eqs 1 and 2, where R = methyl, phenyl



More recently,³ reaction of pyridine thione with $\cdot\text{Cr}(\text{CO})_3\text{Cp}^*$

was shown to result in the formation of an initial tricarbonyl complex that readily lost CO to form a chelated complex



Reaction 3 proceeds not by direct attack on the N–H bond³ but by addition of the chromium radical to the C=S bond of the thione to form an initial activated adduct.⁴

Oxidative addition of the N–H bond at metals has been reported but is relatively rare for first-row transition metal

(4) Crich, D.; Quintero, L. *Chem. Rev.* **1989**, *89*, 1413 and references therein.

* To whom correspondence should be addressed. E-mail: choff@jaguar.ir.miami.edu.

[†] University of Miami.

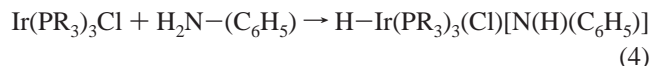
[‡] University of Florida.

(1) Ju, T. D.; Lang, R. F.; Roper, G. C.; Hoff, C. D. *J. Am. Chem. Soc.* **1996**, *118*, 5328.

(2) Ju, T. D.; Capps, K. B.; Lang, R. F.; Roper, G. C.; Hoff, C. D. *Inorg. Chem.* **1997**, *36*, 614.

(3) Sukcharoenphon, K.; Moran, D.; Abboud, K. A.; Schaefer, H. F., III.; Schleyer, P. v. R.; Hoff, C. D., manuscript in preparation.

complexes. Milstein⁵ has investigated N–H activation reactions such as the following



Relatively few examples of N–H oxidative addition to mononuclear complexes have been reported,^{6,7} and those published have been primarily for third-row as opposed to first-row metals. Activation of the N–H bond of ammonia with formation of an NH₂ bridged dimer has also been reported by Milstein.⁸

For polynuclear complexes, prior coordination of an amine might activate the N–H bond to oxidative addition. As part of studies of oxidative addition of the S–H bond, it has been shown that binding to low-valent metals might decrease the thermochemical barrier to oxidative addition of the RS–H bond by as much as ~25–30 kcal/mol.^{1,9} This work reports reactions yielding chromium thiolates of the forms (*o*-HS)-C₆H₄S–Cr(CO)₃Cp* and (*o*-H₂N)C₆H₄S–Cr(CO)₃Cp* in which, unlike the chelating 2-mercaptopyridine ligand shown in eq 3, the potentially chelating ligand is capable of further oxidative addition of S–H and N–H bonds.

Experimental Section

General. Reactions were performed under an argon or carbon monoxide atmosphere using standard glovebox and Schlenk tube techniques. Toluene and heptane were purified by distillation from sodium benzophenone ketyl under argon; methylene chloride by refluxing and subsequent distillation from phosphorus pentoxide. Research-grade carbon monoxide was purchased from Matheson and was used without further purification. FTIR spectra were obtained on a Perkin-Elmer 2000 instrument equipped with microscope/reactor that has been previously described.^{1,2} NMR data were obtained on a Bruker AVANCE 300 MHz NMR spectrometer. Mass spectral data utilizing FAB were acquired on a VG MASS-LAB TRIO-2 spectrometer. Elemental analyses were performed by Galbraith Laboratories, Inc. 2-Aminophenyl disulfide [(2-H₂-NC₆H₄)₂S₂] (recrystallized from slow cooling of a toluene/heptane mixture) and 1,2-benzene dithiol [1,2-C₆H₄(SH)₂] (96%, used as purchased) were obtained from Aldrich Chemical.

Reaction of *Cr(CO)₃Cp* and 1,2-Benzene Dithiol. To a stirred solution of [Cr(CO)₃Cp*]₂ (0.829 g, 1.53 mmol) in 40 mL of toluene under argon was injected 120 μL (1.04 mmol) of 1,2-C₆H₄(SH)₂, and the progress of the reaction was periodically monitored by FTIR spectroscopy. Bands attributed to *Cr(CO)₃Cp* rapidly decreased, as new bands assigned to (*o*-HS)C₆H₄S–Cr(CO)₃Cp* (~2008, 1955, 1920 cm⁻¹) and H–Cr(CO)₃Cp* (1996, 1911 cm⁻¹) grew within minutes of addition. Subsequently, there was a steady increase in bands due to H–Cr(CO)₃Cp* and decrease in bands assigned to (*o*-HS)C₆H₄S–Cr(CO)₃Cp*. No other ν(CO) bands in the infrared region were detected during reaction, in particular none indicative of the chelate {η²-(*o*-HS)C₆H₄S}Cr(CO)₂Cp*. At the end

of reaction (~20 min), FTIR data showed only ν(CO) for the hydride. The reaction mixture was filtered and then concentrated by evaporation in vacuo. With the addition of 35 mL of heptane, cooling at –20 °C over a period of roughly 72 h afforded fine black crystals that were isolated, washed with heptane, and vacuum-dried. Storage of the filtrate in the freezer yielded a second crop of crystals for a total of 0.168 g (50%) of air-stable dimer product. Repeating the procedure in CH₂Cl₂ gave an 80% yield. FAB mass spectroscopic data of an aliquot of a toluene solution of the dimer showed an intense signal for the parent ion (*m/e*): M⁺ = 654, M⁺–Cp* = 519, 1/2M⁺ = 327 (100%). Elemental analysis. Found (calcd) (%): C 58.6 (58.7), H 5.9 (5.9). Qualitative observation of the rate of reaction under either argon or carbon monoxide showed the decay of infrared bands assigned to (*o*-HS)C₆H₄S–Cr(CO)₃Cp* (~2008, 1955, 1920 cm⁻¹) to proceed more rapidly under an argon atmosphere.

Reaction *Cr(CO)₃Cp* and 2-Aminophenyl Disulfide. a. Cr/S = 2/1. To a Schlenk tube containing [Cr(CO)₃Cp*]₂ (0.587 g, 1.08 mmol) and (2-H₂NC₆H₄)₂S₂ (0.138 g, 0.556 mmol) was added 30 mL of toluene under argon. The reaction mixture was periodically monitored by FTIR spectroscopy. Following rapid initial reaction of *Cr(CO)₃Cp*, IR peaks indicative of the formation of (*o*-H₂N)C₆H₄S–Cr(CO)₃Cp* were found (2005, 1946, 1921 cm⁻¹), as well as those assigned to H–Cr(CO)₃Cp* (1996, 1911 cm⁻¹). Careful analysis of the spectroscopic data revealed small bands at 1934 and 1855 cm⁻¹ present as an intermediate complex. The bands were tentatively assigned to the chelate complex {η²-(*o*-H₂N)C₆H₄S}Cr(CO)₂Cp* on the basis of studies performed at a 1/1 Cr/S ratio described below. After approximately 7.5 h, the reaction was judged complete because of full formation of the hydride. Heptane (43 mL) was added, and the sample was stored in a freezer at –20 °C. Over a 3-day period, brown crystals precipitated and were collected and rinsed with heptane. Storage of the filtrate in the freezer yielded a second crop of crystals for a total yield of 0.184 g (55%) of the [{η²-*o*-(μ-NH)C₆H₄S}CrCp*]₂ product. MS in toluene (*m/e*): M⁺ = 620 (100%), M⁺–Cp* = 485, 1/2M⁺ = 310. Elemental analysis. Found (calcd) (%): C 61.4 (61.9), H 6.6 (6.3), N 4.6 (4.5).

b. Cr/S = 1/1. Studies by both IR and NMR (C₆D₆) spectroscopies were performed on this reaction in an identical manner but at a 1/1 Cr/S ratio designed to maximize the formation of (*o*-H₂N)C₆H₄S–Cr(CO)₃Cp*. Under a CO atmosphere, bands (2005, 1946, 1921 cm⁻¹) assigned to this complex were present for a period of days. ¹H NMR data (C₆D₆) were readily collected for (*o*-H₂N)-C₆H₄S–Cr(CO)₃Cp* under these conditions to give δ (ppm) 7.68 (d, 1 H, –SPh), 6.92 (t, 1 H, –SPh), 6.66 (t, 1 H, –SPh), 6.44 (d, 1 H, –SPh), 4.20 (s, 2 H, –NH₂), 1.39 (s, 15 H, –Cp*) (see Figure 1 of the Supporting Information). Evacuation of CO and purging with argon resulted in the appearance of new bands at 1934 and 1855 cm⁻¹ that were assigned to {η²-(*o*-H₂N)C₆H₄S}Cr(CO)₂Cp*. Addition of CO rapidly regenerated (*o*-H₂N)C₆H₄S–Cr(CO)₃Cp*. This process can be repeated several times, but the proposed complex {η²-(*o*-H₂N)C₆H₄S}Cr(CO)₂Cp* appears to be unstable and to decompose slowly in solution. Attempts to obtain NMR data for {η²-(*o*-H₂N)C₆H₄S}Cr(CO)₂Cp* were frustrated by the presence of paramagnetic materials generated during this slow decomposition, which releases CO, thereby converting {η²-(*o*-H₂N)-C₆H₄S}Cr(CO)₂Cp* to {η¹-(*o*-H₂N)C₆H₄S}Cr(CO)₃Cp* as described in relation to FTIR experiments below.

c. Cr/S = 1/1 Followed by Additional Cr. To a 100-mL Schlenk tube containing solid [Cr(CO)₃Cp*]₂ (0.0618 g, 0.114 mmol) and (2-H₂NC₆H₄)₂S₂ (0.0348 g, 0.140 mmol, ~20% excess) was added 20 mL of toluene under an atmosphere of argon. The flask was

(5) Casalnuovo, A. L.; Calabrese, J. C.; Milstein, D. *J. Am. Chem. Soc.* **1988**, *110*, 6738.

(6) Kubas, G. J. *Metal Dihydrogen and σ-Bonded Complexes*; Kluwer Academic: New York, 2001.

(7) Fulton, J. R.; Holland, A. W.; Fox, D. J.; Bergman, R. G. *Acc. Chem. Res.* **2002**, *35*, 44 and references therein.

(8) Schultz, M.; Milstein, D. *J. Chem. Soc., Chem. Commun.* **1993**, 318.

(9) Lang, R. F.; Ju, T. D.; Kiss, G.; Hoff, C. D.; Bryan, J. C.; Kubas, G. *J. Inorg. Chim. Acta* **1997**, *259*, 317.

Table 1. Crystallographic Data and Structure Refinement for $[\{\eta^2\text{-}o\text{-}(\mu\text{-NH})\text{C}_6\text{H}_4\text{S}\}\text{CrCp}^*\}_2]$ and $[\{\eta^2\text{-}o\text{-}(\mu\text{-S})\text{C}_6\text{H}_4\text{S}\}\text{CrCp}^*\}_2]$

	$[\{\eta^2\text{-}o\text{-}(\mu\text{-NH})\text{C}_6\text{H}_4\text{S}\}\text{CrCp}^*\}_2]$	$[\{\eta^2\text{-}o\text{-}(\mu\text{-S})\text{C}_6\text{H}_4\text{S}\}\text{CrCp}^*\}_2]$
Crystal Data		
chemical formula	C ₃₂ H ₄₀ Cr ₂ N ₂ S ₂	C ₃₂ H ₃₈ Cr ₂ S ₄
formula weight	620.78	654.86
crystal system	monoclinic	triclinic
space group	<i>P</i> 2(1)/ <i>n</i>	<i>P</i> $\bar{1}$
<i>a</i> , Å	11.3847(6)	8.0712(3)
<i>b</i> , Å	9.6404(5)	10.3454(4)
<i>c</i> , Å	13.3979(7)	10.7893(5)
α , °	90	62.673(2)
β , °	95.782(2)	70.209(2)
γ , °	90	80.978(2)
<i>V</i> , Å ³	1462.98(13)	753.09(5)
<i>Z</i>	2	1
ρ_{calcd} , mg/m ³	1.409	1.444
μ , mm ⁻¹	0.910	1.020
crystal size, mm	0.19 × 0.17 × 0.15	0.19 × 0.17 × 0.14
color	brown	black
Data Collection		
<i>T</i> , K	193	193
λ , Å	0.710 73	0.710 73
theta range, °	2.24–27.50	2.22–27.48
no. of reflections	12 738	6589
independ. reflections	3356	3335
absorption correction	integration	integration
Solution and Refinement		
solution	direct methods	direct methods
refinement	full-matrix least-squares on <i>F</i> ²	full-matrix least-squares on <i>F</i> ²
data/restraints/param	3356/0/181	3335/0/178
GOF	1.069	1.079
R1 ^a	0.0255	0.0232
wR2 ^b [<i>I</i> > 2 σ (<i>I</i>)]	0.0677	0.0646
largest diff peak, e Å ⁻³	0.353	0.378
largest diff hole, e Å ⁻³	–0.270	–0.372

$$^a \text{R1} = \sum(|F_o| - |F_c|) / \sum|F_o|, \quad ^b \text{wR2} = [\sum(w(F_o^2 - F_c^2)^2) / \sum(w(F_o^2)^2)]^{1/2}.$$

closed and evacuated briefly; then the mixture was stirred vigorously for 30 min. During that time, periodic brief evacuation (to remove any CO present) was performed. An infrared spectrum at that time showed bands consistent with a mixture of *o*-(H₂N)C₆H₄S–Cr(CO)₃Cp* and $\{\eta^2\text{-}o\text{-}(\mu\text{-H}_2\text{N})\text{C}_6\text{H}_4\text{S}\}\text{Cr}(\text{CO})_2\text{Cp}^*$, with no signs of unreacted starting material [Cr(CO)₃Cp*]₂ or H–Cr(CO)₃Cp*. To this solution was added an additional amount of solid [Cr(CO)₃Cp*]₂ (0.0550 g, 0.101 mmol). The flask was again sealed and evacuated. Over a 2-h period, aliquots of this solution were removed at approximately 15-min intervals. Each aliquot removed was placed in the sealed FTIR cell and scanned three times at approximately 5-min intervals. The course of the reaction in the evacuated Schlenk tube showed smooth decreases in the bands assigned to both *o*-(H₂N)C₆H₄S–Cr(CO)₃Cp* and $\{\eta^2\text{-}o\text{-}(\mu\text{-H}_2\text{N})\text{C}_6\text{H}_4\text{S}\}\text{Cr}(\text{CO})_2\text{Cp}^*$ (both species remained present during the reaction), as well as decreases in the bands due to *Cr(CO)₃Cp*. The concentration of H–Cr(CO)₃Cp* increased in parallel with the decrease in starting material. Individual aliquots in the sealed cell (from which released CO cannot escape) showed an *increase* in *o*-(H₂N)C₆H₄S–Cr(CO)₃Cp* and H–Cr(CO)₃Cp*, along with a decrease in $\{\eta^2\text{-}o\text{-}(\mu\text{-H}_2\text{N})\text{C}_6\text{H}_4\text{S}\}\text{Cr}(\text{CO})_2\text{Cp}^*$ and *Cr(CO)₃Cp*. A mass spectrum of an aliquot of the solution at the end of the reaction confirmed the presence of $[\{\eta^2\text{-}o\text{-}(\mu\text{-NH})\text{C}_6\text{H}_4\text{S}\}\text{CrCp}^*\}_2]$. Reactions performed under similar conditions but under a CO atmosphere were qualitatively observed to proceed on a much slower time scale with no detectable amounts of $\{\eta^2\text{-}o\text{-}(\mu\text{-H}_2\text{N})\text{C}_6\text{H}_4\text{S}\}\text{Cr}(\text{CO})_2\text{Cp}^*$ present in solution.

X-ray Crystallographic Experiments

Data Collection. Data were collected at 173 K on a Siemens SMART PLATFORM equipped with a CCD area detector and a

graphite monochromator utilizing Mo K α radiation ($\lambda = 0.710 73$ Å). Cell parameters were refined using up to 8192 reflections. A full sphere of data (1850 frames) was collected using the ω -scan method (0.3° frame width). The first 50 frames were remeasured at the end of data collection to monitor instrument and crystal stability (maximum correction on *I* was <1%). Absorption corrections by integration were applied on the basis of measured indexed crystal faces.

The structure was solved by the direct methods in SHELXTL6 and refined using full-matrix least squares. The non-H atoms were treated anisotropically, whereas the hydrogen atoms were calculated in ideal positions riding on their respective carbon atoms. Crystallographic data and structural refinement for both dimeric structures are summarized in Table 1.

$[\{\eta^2\text{-}o\text{-}(\mu\text{-NH})\text{C}_6\text{H}_4\text{S}\}\text{CrCp}^*\}_2]$. From a reaction of 4 equiv of *Cr(CO)₃Cp* with (2-H₂NC₆H₄)₂S₂ in toluene, a filtered aliquot containing both the chromium hydride and dimer products was layered with 2–3 equiv of heptane by volume in a sealed ampule. No separation of the hydride was needed because of its high solubility in heptane. After a period of 11 days at room temperature, dark crystalline blocks separated from a light-brown solution of the hydride and were isolated, washed with heptane, and stored in degassed mineral oil.

The crystal structure determined is shown in Figure 1, and selected bond lengths and angles are listed in Table 2. The NH proton was located from a difference Fourier map and refined freely. The geometry around the Cr atom is a three-sided pyramid with the Cp* occupying the axial position. A total of 181 parameters were refined in the final cycle of refinement using 3005 reflections with *I* > 2 σ (*I*) to yield R1 and wR2 values of 2.55 and 6.77%, respectively. Refinement was done using *F*².

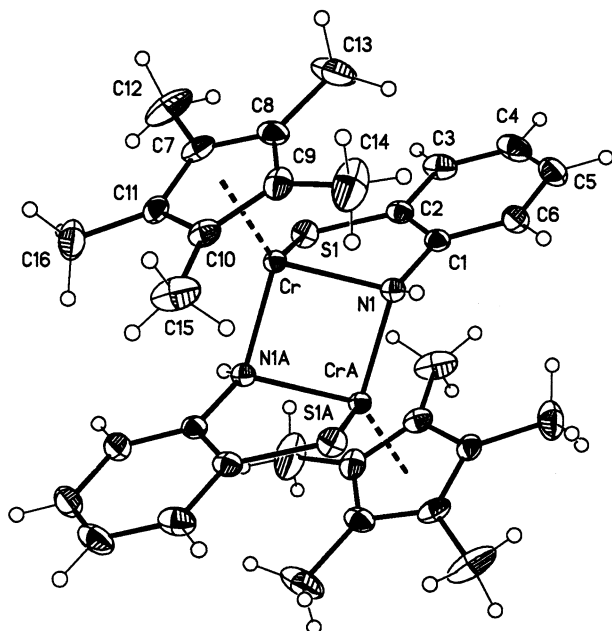


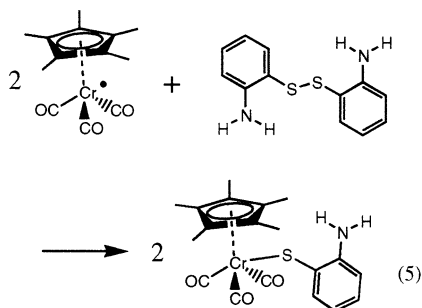
Figure 1. ORTEP diagram of $[\{\eta^2\text{-}o\text{-}(\mu\text{-NH})\text{C}_6\text{H}_4\text{S}\}\text{CrCp}^*]_2$.

$[\{\eta^2\text{-}o\text{-}(\mu\text{-S})\text{C}_6\text{H}_4\text{S}\}\text{CrCp}^*]_2$. In a fashion similar to that described in the previous section, a filtered aliquot of the toluene solution from reaction of 3 equiv of $^*\text{Cr}(\text{CO})_3\text{Cp}^*$ with 1,2- $\text{C}_6\text{H}_4\text{-}(\text{SH})_2$ was layered with 1 equiv of heptane by volume into a sealed glass ampule. The solvent diffusion over a period of 4 days at room temperature yielded dark blocks that were isolated, washed with heptane, and stored in degassed mineral oil.

The crystal structure determined is shown in Figure 2, and selected bond lengths and angles are listed in Table 3. The asymmetric unit consists of a half-dimer located on a center of inversion. A total of 178 parameters were refined in the final cycle of refinement using 3149 reflections with $I > 2\sigma(I)$ to yield R1 and wR2 of 2.32 and 6.46%, respectively. Refinement was done using F^2 .

Results and Discussion

Reaction of $^*\text{Cr}(\text{CO})_3\text{Cp}^*$ with 2-aminophenyl disulfide occurs rapidly to form an initial tricarbonyl complex, as shown in eq 5



Under a CO atmosphere, the aniline thiolate derivative was stable for short periods of time, and it was characterized by

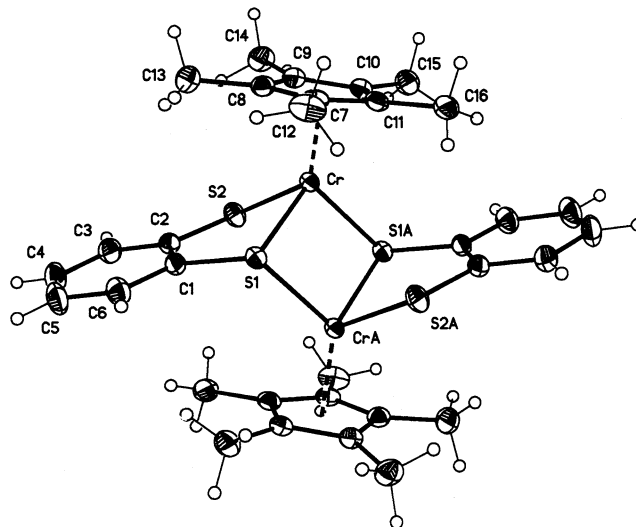
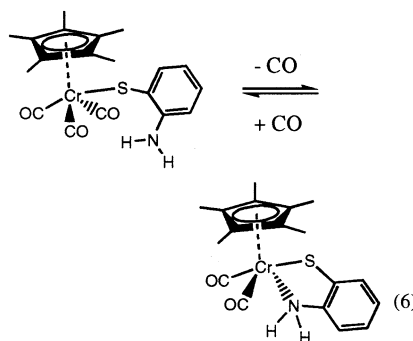


Figure 2. ORTEP diagram of $[\{\eta^2\text{-}o\text{-}(\mu\text{-S})\text{C}_6\text{H}_4\text{S}\}\text{CrCp}^*]_2$.

Table 2. Selected Bond Lengths (Å) and Angles (°) for $[\{\eta^2\text{-}o\text{-}(\mu\text{-NH})\text{C}_6\text{H}_4\text{S}\}\text{CrCp}^*]_2$

Cr—CrA	2.8381(4)	Cr—Cp* (centroid)	1.909(3)
Cr—N1	2.0457(13)	CrA—N1	2.0688(12)
Cr—N1A	2.0688(13)	N1—C1	1.4202(19)
Cr—S1	2.3729(4)	S1—C2	1.7605(16)
N1—H1	0.795(17)		
Cr—N1—CrA	87.22(5)	Cr—N1—C1	112.42(9)
S1—Cr—N1	83.01(4)	Cr—S1—C2	93.50(5)
S1—Cr—N1A	90.76(4)	CrA—N1—C1	123.63(10)
C1—N1—H1	107.1(12)	S1—C2—C1	119.04(11)
Cr—N1—H1	118.8(12)	S1—C2—C3	122.40(13)
CrA—N1—H1	107.5(12)	N1—C1—C2	117.77(13)
N1—Cr—N1A	92.78(5)	N1—C1—C6	122.09(14)

IR, NMR, and MS spectroscopies. Under an atmosphere of argon, the bands at 2005, 1946, and 1921 cm^{-1} (toluene) of the tricarbonyl were replaced by bands at 1934 and 1855 cm^{-1} assigned to the chelating dicarbonyl, as shown in eq 6



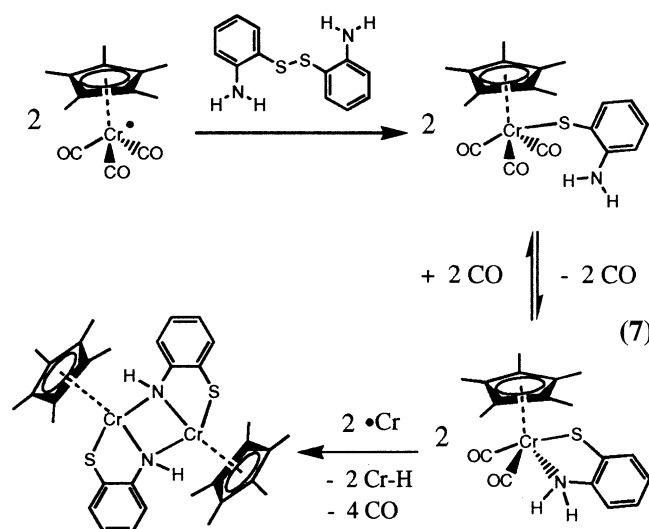
Changing the atmosphere from Ar back to CO regenerated the tricarbonyl complex, indicating that $K_{\text{eq}}^{\text{pCO in atm}} \ll 1$ for reaction 6 because, at 1 atm CO pressure, conversion of formed dicarbonyl to tricarbonyl is quantitative. That is in contrast to the analogous decarbonylation in reaction 3 which

Table 3. Selected Bond Lengths (Å) and Angles (°) for $[\{\eta^2\text{-}o\text{-(}\mu\text{-S)}\text{C}_6\text{H}_4\text{S}\}\text{CrCp}^*\text{]}_2$

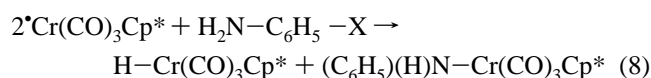
Cr–CrA	3.04	Cr–Cp* (centroid)	1.898(2)
Cr–S1	2.3638 (4)	CrA–S1	2.3816 (4)
Cr–S2	2.3549 (4)	Cr–S1A	2.3816 (4)
S1–C1	1.7806 (14)	S2–C2	1.7561 (14)
S1–Cr–S1A	99.964(12)	S1A–Cr–S2	87.664(14)
S1–Cr–S2	86.504(13)	S1–C2–C1	121.89(10)
Cr–S1–CrA	80.036(12)	S2–C2–C3	119.68(11)
Cr–S2–C2	101.81(5)	S1–C1–C2	120.37(10)
CrA–S1–C1	111.02(5)	S1–C1–C6	119.20(11)
Cr–S1–C1	101.72(5)		

shows no signs of reversibility even under 25 atm CO. Because of its reactivity, $\{\eta^2\text{-}(o\text{-H}_2\text{N})\text{C}_6\text{H}_4\text{S}\}\text{Cr}(\text{CO})_2\text{Cp}^*$ could not be purified.

Solutions containing a mixture of $(o\text{-H}_2\text{N})\text{C}_6\text{H}_4\text{S}\text{-Cr}(\text{CO})_3\text{Cp}^*$ and $\{\eta^2\text{-}(o\text{-H}_2\text{N})\text{C}_6\text{H}_4\text{S}\}\text{Cr}(\text{CO})_2\text{Cp}^*$ react further with $\text{Cr}(\text{CO})_3\text{Cp}^*$. The fact that this reaction is much faster under argon than under carbon monoxide is consistent with attack on the chelating dicarbonyl in the overall scheme shown in eq 7

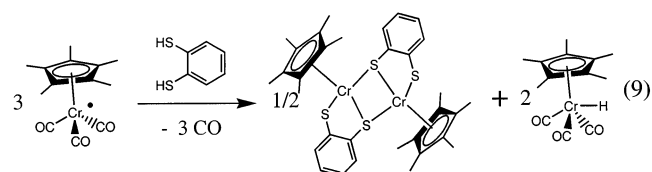


The crystal structure of $[\{\eta^2\text{-}o\text{-(}\mu\text{-NH)}\text{C}_6\text{H}_4\text{S}\}\text{CrCp}^*\text{]}_2$ is shown in Figure 1 and discussed later. The key step in reaction 8 is proposed attack of the Cr radical on the complexed N–H bond. The fact that the oxidative addition reaction is slow under CO atmosphere supports the conclusion that it is the complexed (through the NH₂ group) dicarbonyl and not the uncomplexed tricarbonyl that is reactive. In addition, the chromium radical does not react with the uncomplexed N–H bond of aniline¹⁰



Reaction of $\text{Cr}(\text{CO})_3\text{Cp}^*$ with 1,2- $\text{C}_6\text{H}_4(\text{SH})_2$ was investigated¹¹ several years ago to compare it to reactions of thiophenol as shown in reaction 2. The initial products and

rate were found to be essentially the same as those of thiophenol; however, reaction was found to proceed further to generate additional products. Following an investigation of reaction 7, we reinvestigated the reaction of 1,2- $\text{C}_6\text{H}_4(\text{SH})_2$ with $\text{Cr}(\text{CO})_3\text{Cp}^*$ and found that it proceeded with the net stoichiometry shown in eq 9



The crystal structure of $[\{\eta^2\text{-}o\text{-(}\mu\text{-S)}\text{C}_6\text{H}_4\text{S}\}\text{CrCp}^*\text{]}_2$ is shown in Figure 2 and discussed below. Reaction 9 might follow a mechanism similar to that shown in eq 7. However, because of the more reactive nature of the S–H bond in this system, prior coordination of the S–H bond might not be needed for reaction, and other more complex reaction mechanisms cannot be ruled out.

The structures of $[\{\eta^2\text{-}o\text{-(}\mu\text{-NH)}\text{C}_6\text{H}_4\text{S}\}\text{CrCp}^*\text{]}_2$ and $[\{\eta^2\text{-}o\text{-(}\mu\text{-S)}\text{C}_6\text{H}_4\text{S}\}\text{CrCp}^*\text{]}_2$, (Figures 1 and 2, Tables 1–3) are roughly similar. The four-membered Cr–N–Cr–N and Cr–S–Cr–S ring systems are both essentially planar with dihedral angles of 0; however, the Cr–Cr distances (2.84 and 3.05 Å, respectively) are significantly longer for the S-bridged dimer. The Cr–N–Cr–N unit is nearly a square (angles of 87.22° and 92.78°), whereas the Cr–S–Cr–S complex shows considerable distortion (angles of 99.964° and 80.036°). It is of interest to note that $[\{\eta^2\text{-}o\text{-(}\mu\text{-NH)}\text{C}_6\text{H}_4\text{S}\}\text{CrCp}^*\text{]}_2$, which is bridged through N, could have adopted a S-bridged structure with terminal amido and bridging sulfide groups. The reasons for preference of the NH-bridged over the S-bridged form are not known, and the authors could not find literature data for comparable complexes to provide insight. Several mononuclear and dinuclear structures containing these ligands but with different metals have been reported recently, including $[(\text{Cp}^*\text{Rh})_2(\mu\text{-S})\text{-}1,2\text{-C}_6\text{H}_4\text{S}_2\text{-S,S}']_2$,¹² $[\text{PPN}]\text{Fe}(\text{CO})_2(\text{CN})(\text{S},\text{NH}-\text{C}_6\text{H}_4)$ and $[\text{PPN}]_2[(\text{CN})(\text{CO})_2\text{Fe}(\mu\text{-S},\text{S}-\text{C}_6\text{H}_4)]_2$,¹³ $[\text{CpV}(\eta^2\text{-}\mu\text{-S}_2\text{Ph})_2]_2$,¹⁴ and $[\text{PPN}]_2[\text{W}(\text{CO})_3(\text{NH},\text{S}-\text{C}_6\text{H}_4)]$ and $[\text{PPN}]_2[\text{W}(\text{CO})_4(\text{S},\text{S}-\text{C}_6\text{H}_4)]$.¹⁵ The authors are not aware of comparable dinuclear Cr structures in the literature containing these ligands; however, a number of dinuclear complexes of the formula $[(\eta^5\text{-C}_5\text{R}_5)(\text{Y})\text{Cr}(\mu\text{-X})_2]$ have been reported.¹⁶ Such complexes show Cr–Cr bond distances in the range of 2.6–3.6 Å and, in some cases, antiferromagnetic coupling. The two dimeric complexes discussed here also show antiferro-

(10) Sukcharoenphon, K.; McDonough, J. E.; Hoff, C. D. University of Miami, Coral Gables, FL. Unpublished results.

(11) Ju, T. D. Thermodynamic and Kinetic Studies of Oxidative Addition of Thiols and Disulfides to $\text{Cr}(\text{CO})_3\text{C}_3\text{Me}_5$ and $\text{W}(\text{phen})(\text{CO})_3(\text{EtCN})$. Ph.D. Thesis, University of Miami, Coral Gables, FL, 1996.

(12) Xi, R.; Abe, M.; Suzuki, T.; Nishioka, T.; Isobe, K. *J. Organomet. Chem.* **1997**, *549*, 117.

(13) Liaw, W. F.; Lee, N. H.; Chen, C. H.; Lee, C. M.; Lee, G. H.; Peng, S. M.; *J. Am. Chem. Soc.* **2000**, *122*, 488.

(14) Stephan, D. W. *Inorg. Chem.* **1992**, *31*, 4218.

(15) Darensbourg, D. J.; Draper, J. D.; Frost, B. J.; Reibenspies, J. H. *Inorg. Chem.* **1999**, *38*, 4705.

(16) (a) Pariya, C.; Theopold, K. H. *Curr. Sci.* **2000**, *28*, 1345 and references therein. (b) Hutton, M. A.; Durham, J. C.; Grady, R. W.; Harris, B. E.; Jarrell, C. S.; Mooney, J. M.; Castellani, M. P.; Rheingold, A. L.; Kolle, U.; Korte, B. J.; Sommer, R. D.; Yee, G. T.; Bogges, J. M.; Czernuszewicz, R. S. *Organometallics* **2001**, *20*, 734 and references therein.

magnetic coupling, in addition to a well-resolved ESR spectra in solution. More detailed investigations of the magnetic and spectroscopic properties¹⁷ of these complexes might yield additional insights into the nature of the metal–metal interactions in these dimers.

Conclusion

The H–N(H)(C₆H₅) bond strength (88 kcal/mol¹⁸) is considerably stronger than the H–Cr(CO)₃Cp* bond strength (62 kcal/mol). Free aniline does not react with •Cr(CO)₃Cp* under conditions in which aniline disulfide does react to yield [$\{\eta^2\text{-}o\text{-(}\mu\text{-NH)C}_6\text{H}_4\text{S}\}\text{CrCp}^*\}_2$]. Spectroscopic data support the mechanism shown in eq 7 in which coordination of the pendant NH₂ group serves to activate it to attack by •Cr(CO)₃Cp*. Similar observations were made for related reactions of 1,2-C₆H₄(SH)₂ leading to [$\{\eta^2\text{-}o\text{-(}\mu\text{-S)C}_6\text{H}_4\text{S}\}\text{-CrCp}^*\}_2$]. Reaction of the chelating bis thiol is observed to

occur faster than that of the amino thiol, in keeping with the lower H–S versus H–N bond strength.¹⁷ More detailed kinetic and thermodynamic investigation of these reactions is in progress, but this report (to the authors' knowledge) is the first showing oxidative addition of the N–H bond with •Cr(CO)₃Cp*. This illustrates again, as is well-known in the literature, the powerful role chelation can play in coordinative activation of even strong bonds.

Acknowledgment. Support of this work by the Petroleum Research Fund, administered by the American Chemical Society, is gratefully acknowledged. K.A.A. acknowledges the National Science Foundation and the University of Florida for funding of the purchase of the X-ray equipment.

Supporting Information Available: Tables containing full crystallographic data including bond lengths and angles, thermal parameters, atomic coordinates, and hydrogen-atom parameters for both crystal structures are given (CIF). Figure of NMR spectrum of $\{\eta^1\text{-}(o\text{-H}_2\text{N)C}_6\text{H}_4\text{S}\}\text{Cr(CO)}_3\text{Cp}^*$. This material is available free of charge via the Internet at <http://pubs.acs.org>.

(17) Walker, L.; Angerhofer, A.; Sukcharoenphon, K.; McDonough, E. J.; Hoff, C. D. University of Miami, Coral Gables, FL. Work in progress.

(18) Lide, D. R., Ed. *Handbook of Chemistry and Physics*, 81st ed.; CRC Press: Boca Raton, FL, 2000.

IC0204934